Journal of Sound and Vibration (2003) **259**(5), 1163–1179
doi:10.1006/jsvi.2002.5203, available online at http://www.idealibrary.com on IDEAL®

USING THE CROSS-CORRELATION TECHNIQUE TO EXTRACT MODAL PARAMETERS ON RESPONSE-ONLY DATA

F. Shen, M. Zheng, D. Feng Shi and F. Xu

Institute of Vibration Engineering Research, Nanjing University of Aeronautics and Astronautics, Nanjing, Jiangsu 210016, *People's Republic of China. E-mail: shenfanzm@163.com*

(*Received* 9 *December* 2001, *and in final form* 21 *April* 2002)

Modal parameter identification is used to identify those parameters of the model which describe the dynamic properties of a vibration system. Classical modal parameter extractions usually require measurements of both the input force and the resulting response in laboratory conditions. However, when large-scale operational structures are subjected to random and unmeasured forces such as wind, waves, or aerodynamics, modal parameters estimation must base itself on response-only data. Over the past years, many time-domain modal parameter identification techniques from output-only have been proposed. Among them, the natural excitation technique (NExT) has been a very powerful tool for the modal analysis of structures excited in operating environment. This issue reviews the theoretical development of natural excitation technique (NExT), which uses the cross-correlation functions of measured responses coupling with conventional time-domain parameter extraction under the assumption of white-noise random inputs. Then a frequency-domain poly reference modal identification scheme by coupling the cross-correlation technique with conventional frequency-domain poly reference modal parameter extraction is presented. It uses cross-power spectral density functions instead of frequency response functions and auto- and cross-correlation functions instead of impulse response functions to estimate modal parameters from response-only data. An experiment using an airplane model is performed to investigate the effectiveness of the cross-correlation technique coupled with frequency-domain poly reference modal identification scheme.
© 2002 Elsevier Science Ltd. All rights reserved.

1. INTRODUCTION

Classical modal parameter identifications are usually based on frequency response functions or impulse response functions that require measurements of both the input force and the resulting response. However, for some practical reasons, modal parameter must be extracted only from response data sometimes. For example, for large structures (such as bridges, offshore platforms, and wind turbines), it is very difficult and expensive to measure actual excitation (such as wind, road noise, and wave excitation). The huge amount of energy necessary to induce structural vibrations may cause local damage and excitation becomes very difficult to generate. Additionally, the real operating conditions may differ significantly from the laboratory conditions as the systems are to some extent non-linear or subject to non-linear constraining conditions (e.g., aero-elastic interaction of aircraft in flight) [1]. Sometimes it is not suitable to predict the correct system behavior with the in-laboratory obtained modal models. Therefore, in these applications, the system identification must be done on the basis of response-only data available.

0022-460X/02/$35.00 © 2002 Elsevier Science Ltd. All rights reserved.

The problem of output-only modal analysis has gained considerable attention in recent years. There have been several different approaches to estimate modal parameters from output-only data. They include peak-picking from power spectral density (PSD) functions [2–4], Least-squares curve fitting technique [5, 6], autoregressive moving average (ARMA) models [1, 7–10], the subspace techniques [11–15], and the natural excitation technique (NExT) [16, 17] using cross-correlation functions instead of impulse response functions coupled with some time-domain modal identification schemes such as the random decrement processing with the Ibrahim time-domain (ITD) technique [18], the maximum entropy method (MEM) [6], and the polyreference least-squares complex exponential (PRLSCE) method [1, 11]. The natural excitation technique using cross-correlation functions in time domain has been a very powerful tool for the modal analysis of structures under ambient excitation. However, among them, there are only a limited number of approaches in the frequency domain applicable to modal identification of structures using response data, such as the peak-picking technique to the auto- and cross-power spectra of the operational responses [2–4], and the curve-fitting technique to seek optimal modal parameters [5]. The peak-picking method has been a typical frequency-domain method on response-only, but it suffers from some disadvantages. For example, the modes of the structure should be sufficiently far apart and requires a lot of engineering skills to select the peaks that correspond to system resonances. Although the curve-fitting technique can eliminate these disadvantages, it often meets the minimization problem that is strongly non-linear and methods of linear algebra are not directly applicable to get the solution. In practice, additional assumptions are commonly used to simplify the minimization problem, which usually leads to reduction in the accuracy of the reconstructed eigenvalues and eigenvectors.

The proposed technique in this paper couples the cross-correlation technique with the conventional frequency-domain poly reference parameter extraction to estimate modal parameters from response-only. It uses cross-power spectral density functions between the outputs instead of frequency response functions and auto- and cross-correlation functions instead of impulse response functions to estimate modal parameters from response-only data. The presented scheme has none of the above disadvantages of the peak-picking technique and the curve-fitting technique applied to the power spectra. This issue reviews the theoretical development of natural excitation technique (NExT) and gives how the modal parameters can be determined by the proposed frequency-domain technique for a linear, complex-mode system under the white-noise excitation. An application of the method is presented for an airplane model.

2. THEORETICAL ASPECTS

2.1. THEORETICAL DEVELOPMENT OF NATURAL EXCITATION TECHNIQUE (NEXT)

The following derivation holds for a general class of stationary random inputs. We can describe the behavior of the system by the equations of motion [16]:

$$[M]\{\ddot{y}(t)\} + [C]\{\dot{y}(t)\} + [K]\{y(t)\} = \{f(t)\}, \tag{1}$$

where $[M]$ is the mass matrix, $[C]$ is the damping matrix, $[K]$ is the stiffness matrix, $\{f(t)\}$ is the vector of random forcing function, $\{y(t)\}$ is the vector of random displacements.

Let us introduce

$$[M]\{\dot{y}(t)\} - [M]\{\dot{y}(t)\} = \{0\}. \tag{2}$$

Combining equation (1) with equation (2) results in the state-space model corresponding to the dynamic equations [15]:

$$[A]\{\dot{Y}(t)\} + [B]\{Y(t)\} = \{F(t)\}, \tag{3}$$

where

$$[A] = \begin{bmatrix} [C] & [M] \\ [M] & [0] \end{bmatrix}, [B] = \begin{bmatrix} [K] & [0] \\ [0] & -[M] \end{bmatrix}, \{Y(t)\} = \begin{Bmatrix} \{y(t)\} \\ \{\dot{y}(t)\} \end{Bmatrix}, \{F(t)\} = \begin{Bmatrix} \{f(t)\} \\ \{0\} \end{Bmatrix}.$$

We can use a modal transformation:

$$\{Y(t)\} = [\phi]\{q(t)\} = \begin{bmatrix} [\psi] \\ [\psi][\Lambda] \end{bmatrix}\{q(t)\}, \tag{4}$$

where $[\phi]$ is the $2N_m \times 2N_m$ complex modal matrix, $\{q(t)\}$ is the $2N_m \times 1$ vector of modal co-ordinates, $[\psi]$ is the $N_m \times 2N_m$ mode shape matrix, $[\Lambda]$ is the $2N_m \times 2N_m$ complex eigenvalue matrix, N_m is the number of system d.o.f..

Then we can derive

$$\{y(t)\} = [\psi]\{q(t)\} = \sum_{r=1}^{2N_m} \{\psi_r\} q_r(t), \tag{5}$$

where $\{\psi_r\}$is the vector of the rth mode shape, $q_r(t)$ is the rth component of vector $\{q(t)\}$.

We use the orthogonality of mode shapes

$$[\phi]^{\mathrm{T}}[A][\phi] = [a], \quad [\phi]^{\mathrm{T}}[B][\phi] = [b], \tag{6}$$

where $^{\mathrm{T}}$ denotes the transpose, $[a]$, $[b]$ are diagonal matrices.

Premultiplying equation (3) by $[\phi]^{\mathrm{T}}$ gives

$$[\phi]^{\mathrm{T}}[A]\{\dot{Y}(t)\} + [\phi]^{\mathrm{T}}[B]\{Y(t)\} = [\phi]^{\mathrm{T}}\{F(t)\}. \tag{7}$$

Substituting equation (4) into equation (7) results in the following:

$$[\phi]^{\mathrm{T}}[A][\phi]\{\dot{q}(t)\} + [\phi]^{\mathrm{T}}[B][\phi]\{q(t)\} = [\phi]^{\mathrm{T}}\{F(t)\}. \tag{8}$$

A set of scalar equations in the modal co-ordinates can be given as follows:

$$a_r\dot{q}_r(t) + b_r q_r(t) = \{\psi_r\}^{\mathrm{T}}\{f(t)\}, \tag{9}$$

where a_r, b_r are the elements of diagonal matrices $[a]$, $[b]$.

The solution of equation (9) can be obtained from Duhamel integral assuming zero initial conditions:

$$q_r(t) = \frac{1}{a_r}\int_{-\infty}^{t} \{\psi_r\}^{\mathrm{T}}\{f(\tau)\}\mathrm{e}^{\lambda_r(t-\tau)}\,\mathrm{d}\tau, \tag{10}$$

where $\lambda_r = -b_r/a_r$.

Equations (5) and (10) can now be used to obtain the solution for $\{y(t)\}$:

$$\{y(t)\} = \sum_{r=1}^{2N_m} \frac{1}{a_r}\{\psi_r\}\int_{-\infty}^{t} \{\psi_r\}^{\mathrm{T}}\{f(\tau)\}\mathrm{e}^{\lambda_r(t-\tau)}\,\mathrm{d}\tau. \tag{11}$$

The response $y_{nl}(t)$ at the nth d.o.f. due to a single input force $f_l(t)$ at the lth d.o.f. can be derived as

$$y_{nl}(t) = \sum_{r=1}^{2N_m} \frac{1}{a_r}\psi_{nr}\psi_{lr}\int_{-\infty}^{t} f_l(\tau)\mathrm{e}^{\lambda_r(t-\tau)}\,\mathrm{d}\tau, \tag{12}$$

where ψ_{nr} is the nth component of the rth mode shape vector $\{\psi_r\}$.

Define the cross-correlation function $R_{npl}(T)$ as the expected value of the product of two stationary responses $y_{nl}(t)$ and $y_{pl}(t)$ due to the single input at the lth d.o.f. evaluated at a time separation of T [18]:

$$R_{npl}(T) = E[y_{nl}(t+T)y_{pl}(t)], \tag{13}$$

where E is the expectation operator.

Substituting equation (12) into equation (13) results in the following:

$$R_{npl}(T) = \sum_{r=1}^{2N_m}\sum_{s=1}^{2N_m}\frac{1}{a_r a_s}\psi_{nr}\psi_{lr}\psi_{ps}\psi_{ls}\int_{-\infty}^{t}\int_{-\infty}^{t+T}\mathrm{e}^{\lambda_r(t+T-\sigma)}\,\mathrm{e}^{\lambda_s(t-\tau)}E[f_l(\sigma)f_l(\tau)]\,\mathrm{d}\sigma\,\mathrm{d}\tau. \tag{14}$$

Assuming $f_l(t)$ is white noise, then

$$E[f_l(\sigma)f_l(\tau)] = \alpha_l\delta(\tau-\sigma), \tag{15}$$

where α_l is a constant and $\delta(t)$ is the Dirac delta function.

Substituting equation (15) into equation (14) and collapsing the integration produces the following:

$$R_{npl}(T) = \sum_{r=1}^{2N_m}\sum_{s=1}^{2N_m}\frac{\alpha_l\psi_{nr}\psi_{lr}\psi_{ps}\psi_{ls}}{a_r a_s(-\lambda_r-\lambda_s)}\,\mathrm{e}^{\lambda_r T}. \tag{16}$$

Summing over all the inputs $f_l(t), l = 1, 2, \ldots, L$, which are assumed to be uncorrelated with one another, we can get the cross-correlation function $R_{np}(T)$ between the output n and the output p:

$$R_{np}(T) = \sum_{r=1}^{2N_m}\psi_{nr}Q_{pr}\,\mathrm{e}^{\lambda_r T}, \tag{17}$$

where Q_{pr} is a new constant defined by

$$Q_{pr} = \sum_{s=1}^{2N_m}\sum_{l=1}^{L}\frac{-\alpha_l\psi_{lr}\psi_{ps}\psi_{ls}}{a_r a_s(\lambda_r+\lambda_s)}. \tag{18}$$

It shows that the cross-correlation function in equation (17) is a sum of complex exponential functions of the same form as the impulse response function of the original system in the following:

$$h_{nl}(t) = \sum_{r=1}^{2N_m}\psi_{nr}W_{lr}\,\mathrm{e}^{\lambda_r t}, \tag{19}$$

where $h_{nl}(t)$ is the impulse response at point n due to the input force at point l, W_{lr} is the modal participation factor.

Consequently, the classical modal parameter techniques using impulse response functions as input like eigensystem realization algorithm (ERA) and poly-reference least-squares complex exponential (PRLSCE) method are appropriate to extract the modal parameters from response-only. This technique is generally referred to as NExT [16].

2.2. POWER SPECTRAL DENSITY FUNCTIONS WITH THE SAME FORM AS FREQUENCY RESPONSE FUNCTIONS

The Fourier transform of the impulse response function $h_{nl}(t)$ in equation (19) can be performed, then the frequency response function $H_{nl}(\mathrm{j}\omega)$ can be expressed as follows:

$$H_{nl}(\mathrm{j}\omega) = \sum_{r=1}^{2N_m} \frac{\psi_{nr} W_{lr}}{\mathrm{j}\omega - \lambda_r}. \tag{20}$$

The cross-power spectral density function $G_{np}(\mathrm{j}\omega)$ is the Fourier transform of the cross-correlation function $R_{np}(T)$ in equation (17), and can be expressed as

$$G_{np}(j\omega) = \sum_{r=1}^{2N_m} \frac{\psi_{nr} Q_{pr}}{j\omega - \lambda_r}. \tag{21}$$

It can be easily shown that the cross-power spectral density function in equation (21) is a sum of fraction functions of the same form as the frequency response function of the original system in equation (20). Each fraction has a pole that implies a natural frequency and damping ratio corresponding to a structural mode, and the residue $\psi_{nr} Q_{pr}$ in equation (21) and $\psi_{nr} W_{lr}$ in equation (20) are proportional to the nth component ψ_{nr} of the mode shape $\{\psi_r\}$. It is well known that the term $\psi_{nr} W_{lr}$ in the frequency response function in equation (20) can be identified as the mode shape component. When the input forces are not measurable, the residue $\psi_{nr} Q_{pr}$ in equation (21) can be used to derive the complete mode shape by selecting a common reference station p to eliminate the term Q_{pr}. Consequently, the cross-power spectral density functions between responses can be used to estimate modal parameters from output-only instead of frequency response functions in frequency-domain modal identifications.

2.3. THE FREQUENCY-DOMAIN POLY-REFERENCE MODAL EXTRACTION FROM RESPONSE-ONLY

In conventional modal analysis, the frequency-domain poly-reference modal identification using frequency response functions [19] is a well-known technique to derive global estimates of modal parameters.

From equation (19), we obtain the impulse response function matrix at N response stations due to force inputs at points $1, 2, \ldots, L$:

$$[h(t)] = [\psi][\mathrm{e}^{\Lambda t}][W], \tag{22}$$

where $[h(t)]$ is the impulse response function matrix, $[W]$ is the modal participation factor matrix.

We can get the first derivatives of the above equation as

$$[\dot{h}(t)] = [\psi][\Lambda][\mathrm{e}^{\Lambda t}][W]. \tag{23}$$

The Laplace transform of equations (22) and (23) can be, respectively, derived as

$$[H(s)] = [\psi](s[I] - [\Lambda])^{-1}[W] \tag{24}$$

and

$$[\dot{H}(s)] = [\psi][\Lambda](s[I] - [\Lambda])^{-1}[W], \tag{25}$$

where $[H(s)]$ is the transfer function matrix, $[I]$ is a unit matrix.

Let us constitute a new matrix equation with equations (24) and (25) as

$$\begin{bmatrix} [H(s)] \\ [\dot{H}(s)] \end{bmatrix} = \begin{bmatrix} [\psi] \\ [[\psi][\Lambda]] \end{bmatrix} (s[I] - [\Lambda])^{-1}[W] = [\phi][O(s)], \tag{26}$$

where $[O(s)] = (s[I] - [\Lambda])^{-1}[W]$.

In this method, a system matrix $[X]$ is defined so that it satisfies

$$[X][\psi]+[\psi][\Lambda]=[0]. \tag{27}$$

It can be rewritten as

$$[[X]\vdots[I]]\begin{bmatrix}[\psi]\\ [\psi][\Lambda]\end{bmatrix}=[[X]\vdots[I]][\phi]=[0]. \tag{28}$$

Postmultiplying the above equation by $[O(s)]$, according to equation (26), we can obtain

$$[[X]\vdots[I]][\phi][O(s)]=[[X]\vdots[I]]\begin{bmatrix}[H(s)]\\ [\dot{H}(s)]\end{bmatrix}=[0]. \tag{29}$$

Equation (29) can also be expressed in the following way:

$$[X][H(s)]+[\dot{H}(s)]=[0]. \tag{30}$$

According to the following relationship

$$[\dot{H}(s)]=s[H(s)]-[h(t)]|_{t=0}. \tag{31}$$

Equation (30) can be written as

$$[X][H(s)]+s[H(s)]-[h(t)]|_{t=0}=[0]. \tag{32}$$

Let $s=\mathrm{j}\omega$, we can get

$$[X][H(\mathrm{j}\omega)]+\mathrm{j}\omega[H(\mathrm{j}\omega)]-[h(t)]|_{t=0}=[0], \tag{33}$$

where $[H(\mathrm{j}\omega)]$ is the frequency response function matrix.

It has been shown that, under the assumption that the system is excited by stationary white noise, cross-correlation functions between the outputs have the same form as impulse response functions and power spectral density functions as frequency response functions. Subsequently, the frequency-domain poly-reference modal identification is appropriate to extract the modal parameters from response-only data measured under operational conditions by using the power spectral densities of responses instead of frequency response functions and cross-correlation functions instead of impulse response functions.

Define the auto- and cross-correlation function matrix $[R(T)]$ between N and P responses which serve as references as

$$[R(T)]=\begin{bmatrix}R_{11}(T) & R_{12}(T) & \cdots & R_{1P}(T)\\ R_{21}(T) & R_{22}(T) & \cdots & R_{2P}(T)\\ \vdots & \vdots & \vdots\ \vdots & \vdots\\ R_{N1}(T) & R_{N2}(T) & \cdots & R_{NP}(T)\end{bmatrix}. \tag{34}$$

Equations (17) and (34) can now be used to obtain

$$[R(T)]=[\psi][\mathrm{e}^{\Lambda T}][Q], \tag{35}$$

where $[Q]$ is a constant matrix filled up with the term Q_{pr} and at $T=0$, the following results:

$$[R(T)]|_{T=0}=[\psi][Q]. \tag{36}$$

From the Fourier transform of equation (35), we also can get

$$[G(\mathrm{j}\omega)]=[\psi](\mathrm{j}\omega[I]-[\Lambda])^{-1}[Q], \tag{37}$$

where $[G(j\omega)]$ is the auto- and cross-power spectral density function matrix of measured responses.

Using the cross-power spectral density function matrix $[G(j\omega)]$ instead of the frequency response function matrix $[H(j\omega)]$ and the auto- and cross-correlation function matrix $[R(T)]$ instead of the impulse response function matrix $[h(t)]$ in equation (33), the following results:

$$[X][G(j\omega)] + j\omega[G(j\omega)] - [R(T)]|_{T=0} = [0]. \tag{38}$$

Substituting equation (36) into equation (38), we can get

$$[X][G(j\omega)] + j\omega[G(j\omega)] - [\psi][Q] = [0]. \tag{39}$$

An over-determined set of equations can be obtained for all discrete frequencies $\omega_1, \omega_2, \ldots, \omega_K$ in the frequency range of measurement:

$$[X][G(j\omega_1)] - [\psi][Q] = -j\omega_1[G(j\omega_1)], \tag{40}$$

$$[X][G(j\omega_2)] - [\psi][Q] = -j\omega_2[G(j\omega_2)], \tag{41}$$

$$[X][G(j\omega_K)] - [\psi][Q] = -j\omega_K[G(j\omega_K)]. \tag{42}$$

These equations can also be written as

$$[[X]\vdots - [\psi][Q]]\begin{bmatrix} [D] \\ [\,[I] \quad [I] \quad \ldots \quad [I]\,] \end{bmatrix} = [D][\Omega], \tag{43}$$

where

$$[D] = \big[\,[G(j\omega_1)] \quad [G(j\omega_2)] \quad \ldots \quad [G(j\omega_K)]\,\big],$$

$$[\Omega] = -\mathrm{diag}\big[\,j\omega_1[I] \quad j\omega_2[I] \quad \ldots \quad j\omega_K[I]\,\big].$$

From equation (43), we can get

$$[V] = [[X]\vdots - [\psi][Q]] = [D][\Omega]\begin{bmatrix} [D] \\ [\,[I] \quad [I] \quad \ldots \quad [I]\,] \end{bmatrix}^{+}, \tag{44}$$

where + denotes the generalized inverse. The matrix $[V]$ can be obtained in a least-squares sense by considering all available of the measured power spectral densities. The matrix $[X]$ is given by the first N columns of matrix $[V]$, and the negative of matrix $[\psi]$ $[Q]$ is given by the last P columns (from $N+1$ to $N+P$) of matrix $[V]$.

According to equation (27), an eigenvalue problem can be formulated as

$$[X]\{\psi_r\} + \lambda_r\{\psi_r\} = \{0\}. \tag{45}$$

Once the system matrix $[X]$ is known, in the case of complex conjugate pairs being considered, $2N$ complex eigenvalues λ_r and $2N$ complex eigenvector $\{\psi_r\}$ can be obtained from equation (45). The poles λ_r of the original vibrating system can be used to obtain the damped natural frequency ω_{nr} by the following equation:

$$\omega_{nr} = \sqrt{R_e(\lambda_r)^2 + I_m(\lambda_r)^2}. \tag{46}$$

And the damping ratio ξ_r of the rth mode can be given by

$$\xi_r = -\frac{R_e(\lambda_r)}{\omega_{nr}}, \tag{47}$$

where $R_e(\cdot)$ denotes the real part, $I_m(\cdot)$ denotes the imaginary part.

The rth eigenvector $\{\psi_r\}$ corresponding to the eigenvalue λ_r of the system matrix $[X]$ is just the rth mode shape of the vibrating system.

2.4. POWER SPECTRAL DENSITY SYNTHESIS

Equation (39) can be expressed as follows:

$$([X] + \mathrm{j}\omega[I])[G(\mathrm{j}\omega)] = [\psi][Q]. \tag{48}$$

Let $[J] = [\psi][Q]$, the auto- and cross-power spectral density matrix $[G(\mathrm{j}\omega)]$ between the outputs can be written as

$$[G(\mathrm{j}\omega)] = ([X] + \mathrm{j}\omega[I])^{+}[\mathrm{J}]. \tag{49}$$

It can be easily shown that matrix $[G(\mathrm{j}\omega_1)], [G(\mathrm{j}\omega_2)], \ldots, [G(\mathrm{j}\omega_K)]$ can be derived from equation (49) by considering all frequencies in the selected frequency interval. Therefore, it can be used to graphically check the quality of the output-only modal model by overlaying the actual test data with the synthesized data.

2.5. REDUCTION OF MODEL ORDER

In some applications, the number of measured locations N is often greater than the number of system modes N_e in the frequency range of interest. When matrix $[V]$ is obtained from equation (43), it will be time and core storage consuming and lead to the spurious modes. Therefore, the selection of model order should be done to solve this problem. Inspection of the singular values [20] might be helpful for finding the correct model order in the proposed frequency-domain modal identification.

Define a co-ordinate square difference matrix as

$$[Z] = \sum_{k=1}^{K} R_e([G(\mathrm{j}\omega_k)]\ [G^{\mathrm{H}}(\mathrm{j}\omega_k)]), \tag{50}$$

where $^{\mathrm{H}}$ denotes the complex conjugate and matrix transpose.

Performing an SVD decomposition on matrix $[Z]$ gives the following:

$$[Z] = [U][\Sigma][S]^{\mathrm{T}} = \begin{bmatrix}[U_1] & [U_2]\end{bmatrix}\begin{bmatrix}[\Sigma_1] & [0]\\ [0] & [0]\end{bmatrix}\begin{bmatrix}[S_1]^{\mathrm{T}}\\ [S_2]^{\mathrm{T}}\end{bmatrix} = [U_1][\Sigma_1][S_1]^{\mathrm{T}}, \tag{51}$$

where $[\Sigma_1]$ contains N_e non-zero singular values in descending order with

$$[\Sigma_1] = \mathrm{diag}[\varepsilon_1\varepsilon_2\ldots\varepsilon_{Ne}], \quad \varepsilon_1 \geqslant \varepsilon_2 \ldots \varepsilon_{Ne} > 0, \tag{52}$$

$[U_1]$ is an $N \times N_e$ matrix which contains the singular vectors corresponding to non-zero singular values, $[U_2]$ is an $N \times (N - N_e)$ matrix which contains the singular vectors corresponding to zero singular values. The model order is estimated as N_e by truncating the singular values. In practice, the engineer often select N_e such that $\varepsilon_{Ne} \gg \varepsilon_{Ne+1}$.

Matrix $[U_1]^{\mathrm{T}}$ can be used to reduce the order of power spectral density matrix $[G(\mathrm{j}\omega)]$ as the following:

$$[G(\mathrm{j}\omega)]_{redu} = [U_1]^{\mathrm{T}}[G(\mathrm{j}\omega)], \tag{53}$$

where $[G(\mathrm{j}\omega)]_{redu}$ is a matrix with dimension $N_e \times P$. In practical computing, feeding order-reduced matrix $[G(\mathrm{j}\omega)]_{redu}$ instead of matrix $[G(\mathrm{j}\omega)]$ in equation (44) allows to obtain order-reduced system matrix $[X]_{redu}$ with dimension $N_e \times N_e$. Solving an eigenvalue problem of matrix $[X]_{redu}$ can lead to the evaluations of $2N_e$ discrete complex eigenvalues and $2N_e$ complex eigenvectors in the case of complex conjugate pairs being considered.

The eigenvalues λ_r can be used to estimate the damped natural frequency ω_{nr} and the damping ratio ξ_r of the original vibrating system according to equations (46) and (47).

Substituting equation (37) into equation (53) produces the following:

$$[G(j\omega)]_{redu} = [U_1]^{\mathrm{T}}[\psi](j\omega[I] - [\Lambda])^{-1}[Q] = [\psi]_{redu}(j\omega[I] - [\Lambda])^{-1}[Q], \tag{54}$$

where $[\psi]_{redu}$ is the order-reduced eigenvector matrix.

We can get

$$[\psi]_{redu} = [U_1]^{\mathrm{T}}[\psi]. \tag{55}$$

The mode shape matrix $[\psi]$ of the vibrating system at the sensor locations can be given by

$$[\psi]^{\mathrm{T}} = [\psi_{redu}]^{\mathrm{T}}[U_1]^{+}. \tag{56}$$

Sometimes the criteria of an SVD technique is not of great use as a drop or a break between singular values is not apparent in practice. Other techniques such as stabilization diagrams are needed in order to find the correct model order.

3. APPLICATION

In this context, a case study was performed employing the data acquired from a test conducted on an airplane model in order to assess the usefulness of the algorithm described above for modal identification from response-only.

3.1. DESCRIPTION OF TEST STRUCTURE AND TESTS

The airplane model is made of aluminum and the fuselage is 1000 mm long and the wingspan 1100 mm wide. It was suspended on three flexible threads at the fuselage. The responses were measured only in the vertical direction at 24 points for vertical excitation at two symmetrical excitation points. Figure 1 shows the distribution of the 24 acceleration transducers.

Two uncorrelated white noise signals were applied to the 2 shakers. Figure 2 shows the auto-power spectral densities of the two input forces, revealing that the actual excitation was not perfectly flat due to the interaction between shaker and structure. The MVMAS-3 multi-vibration measurement and analysis system with 64 input channels was employed to

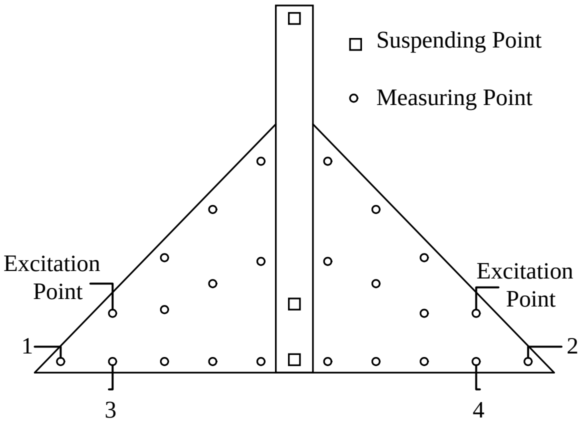

Figure 1. The airplane model with indication of the distribution of transducers.

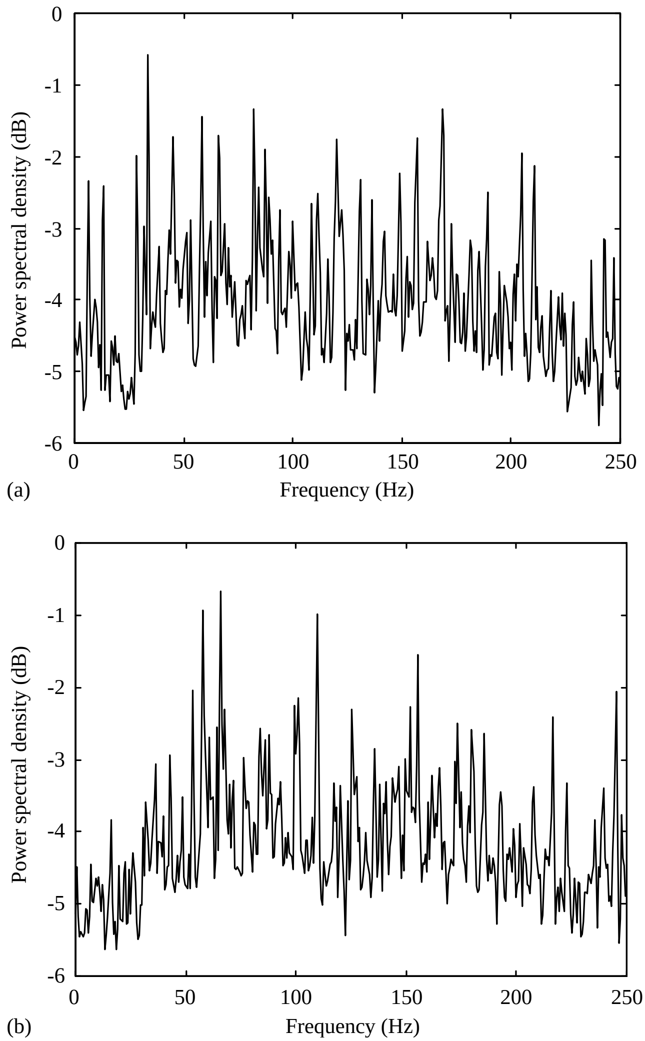

Figure 2. Auto-power spectral density of the input forces. (a) The auto-power spectral density of left input force and (b) the auto-power spectral density of right input force.

acquire the response data at the 24 locations with a sampling rate of 512 Hz, which results in a bandwidth of 0–200 Hz. The responses from 24 acceleration transducers were converted into displacement response signals by computing. Then all the responses were chosen as reference points and the auto- and cross-power spectral densities of all the responses were calculated for the output-only modal analysis, which enables a global estimate of modal parameters of the structure. The segment size equaled 1024 and no overlap was used. A Hanning window was used to avoid leakage, and about 40 averages were performed for 40 960 data samples corresponding to a signal duration of 80 s. The singular value truncation technique was used to reduce the model order when the number of measured locations is greater than the number of modes. The order-reduced cross-power spectral density matrix was fed to the technique presented in this paper to extract the modal parameters from output-only.

The modal parameters were obtained using multi-point pure mode excitation technique, yielding the baseline model for comparison purposes.

3.2. TEST RESULTS

In the frequency range 0–200 Hz, the break in singular values of matrix $[Z]$ occurs between 18 and 19 as shown in Figure 3. It can also be seen from Table 1 that the largest ratio of two adjacent singular values is 13·533 between 18 and 19 but the others are much less. The order of the model in the presented scheme can be considered as 18. However, sometimes the inspection of singular values does not show a significant drop, and this information will have an influence upon the selection of system mode number in the interested frequency range. A lower value for the model order will result in omitted system modes. When the number of the model order is chosen higher than the number of true modes, the spurious modes will be introduced and the computational load will increase. In this case, other techniques such as stabilization diagrams are then needed to help finding the correct model order.

Table 2 lists the results for all found modes without counting the rigid-body modes from both multi-point pure mode excitation technique and the presented frequency-domain poly-reference modal identification with power spectral densities. In addition to the frequencies and damping ratios, the modal assurance criterion MAC-value between the mode shapes extracted by multi-point pure mode excitation method and the mode shapes extracted by the technique described above are given. Both the frequencies and

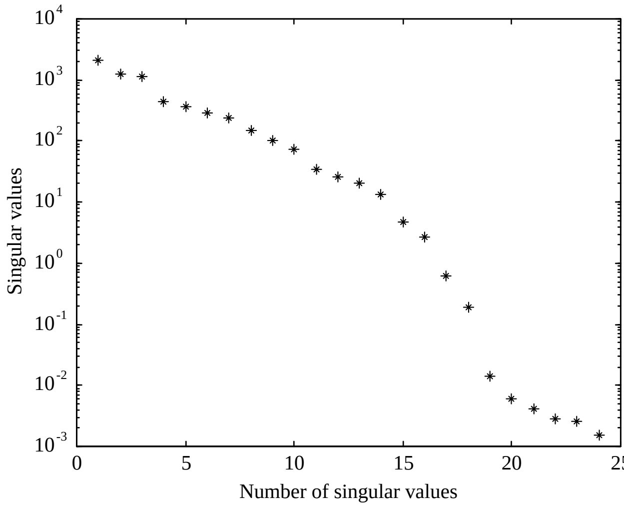

Figure 3. Singular values of coordinate square difference matrix $[Z]$.

TABLE 1

Singular values of co-ordinate square difference matrix $[Z]$

No.	1	2	3	4	5	6	7	8
Singular value	2095·4	1229·0	1115·0	437·4	357·9	286·1	233·9	147·7
No.	9	10	11	12	13	14	15	16
Singular value	101·5	72·9	34·3	25·9	20·0	13·5	4·72	2·62
No.	17	18	19	20	21	22	23	24
Singular value	0·61	0·19	0·014	0·0062	0·0042	0·0028	0·0026	0·0015

Table 2

Comparison of modal parameters from two different techniques

Mode no.	Symmetry/ antisymmetry	Multi-point pure mode excitation method		Frequency-domain modal identification technique from output-only		
		Freq. (Hz)	Damping (%)	Freq. (Hz)	Damping (%)	MAC (%)
1	S	14·8	5·14	15·3	4·76	98·2
2	A	23·6	0·86	24·2	0·36	99·1
3	A	35·1	4·25	36·2	4·05	98·6
4	S	45·0	1·67	44·9	2·01	99·2
5	A	52·5	3·11	52·4	3·53	98·4
6	S	63·4	1·50	64·7	1·61	99·0
7	A	69·2	1·45	69·6	1·70	96·7
8	S	74·8	6·56	75·3	5·05	83·2
9	A	91·5	1·02	92·3	1·35	92·1
10	S	98·7	1·36	97·6	0·92	98·8
11	A	107·3	0·93	107·3	0·96	89·3
12	A	112·9	1·58	111·7	1·05	90·9
13	S	143·5	0·70	143·4	0·82	96·5
14	S	151·5	0·39	150·7	0·64	98·8
15	A	158·3	0·48	158·2	0·39	99·0
16	S	170·2	1·05	170·8	0·88	97·6
17	A	173·3	0·54	173·4	0·52	82·5
18	S	185·5	0·50	186·2	0·67	96·8

MAC-values between the mode shapes have a good agreement with the baseline model in Table 2. But the damping ratio of some modes obtained from the two techniques have much differences, such as a damping of 0·86% with the multi-point pure mode excitation method but 0·36% with the proposed method in the second mode. It may be difficult to identify the reasonably accurate damping ratios in all modes from response-only using the outlined frequency-domain method in the paper. A pair of closely spaced modes whose frequencies are around 170 and 173 Hz were well extracted. The first 4 mode shapes obtained from two different modal identification approaches are visualized in an airplane model in Figure 4. The left results come from multi-point pure mode excitation method and the right from the frequency-domain poly-reference modal parameter extraction.

The auto- and cross-power spectral densities between responses were fitted by using eighteen identified poles in the frequency band 0–200 Hz. Synthesized auto- and cross-power spectral densities of the responses are overlaid with actual measured auto- and cross-power spectral density data in Figure 5, which shows a good agreement. The dashed lines correspond to the measured power spectral densities, and the solid lines show the synthesized power spectral densities. The plot illustrates how the synthesis of data can be used to validate the modal model.

4. CONCLUSION

The paper aims to present a modal identification technique from output-only data based on coupling the cross-correlation technique with conventional frequency-domain poly-reference modal identifications. It uses the auto- and cross-power spectral density functions between the measured responses instead of frequency response functions and

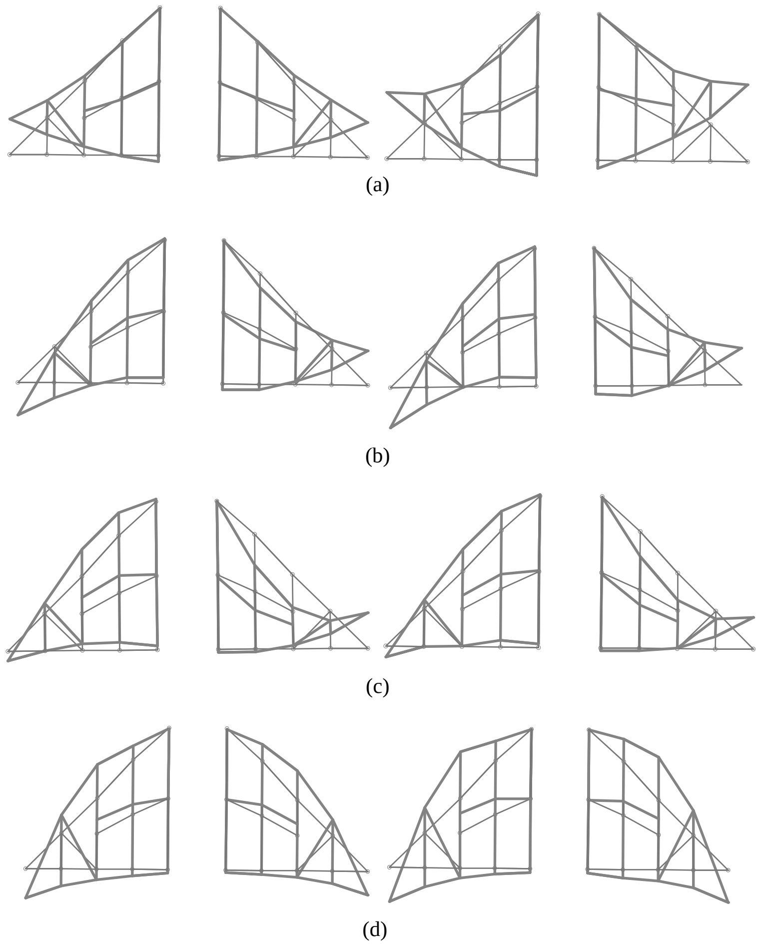

(Left: Multi-point pure mode excitation method   Right: Presented frequency-domain technique)

Figure 4. Comparison of mode shapes from two different methods. (a) The first mode shape from two different methods; (b) the second mode shape from two different methods; (c) the third mode shape from two different methods and (d) the fourth mode shape from two different methods.

auto- and cross-correlation functions instead of impulse response functions under the assumption of white-noise input forces. When applied to an experiment using an airplane model, it yielded good results. The procedure to solve the problem of a vibrating system from output-only data is divided into three parts:

(a) Acquire response data from the operating structure under relatively stationary operating conditions. Long-time series of response data are desired to allow significant averaging of the data.
(b) Calculate auto- and cross-power spectral densities from these time histories. The cross-powers of each output channel will be calculated with respect to a subset of the output channels that function as references.
(c) Use the frequency-domain poly reference modal identification scheme to extract the modal parameters from output-only data by treating the auto- and cross-power spectral density functions of responses instead of frequency response functions in the traditional frequency-domain modal parameter extraction.

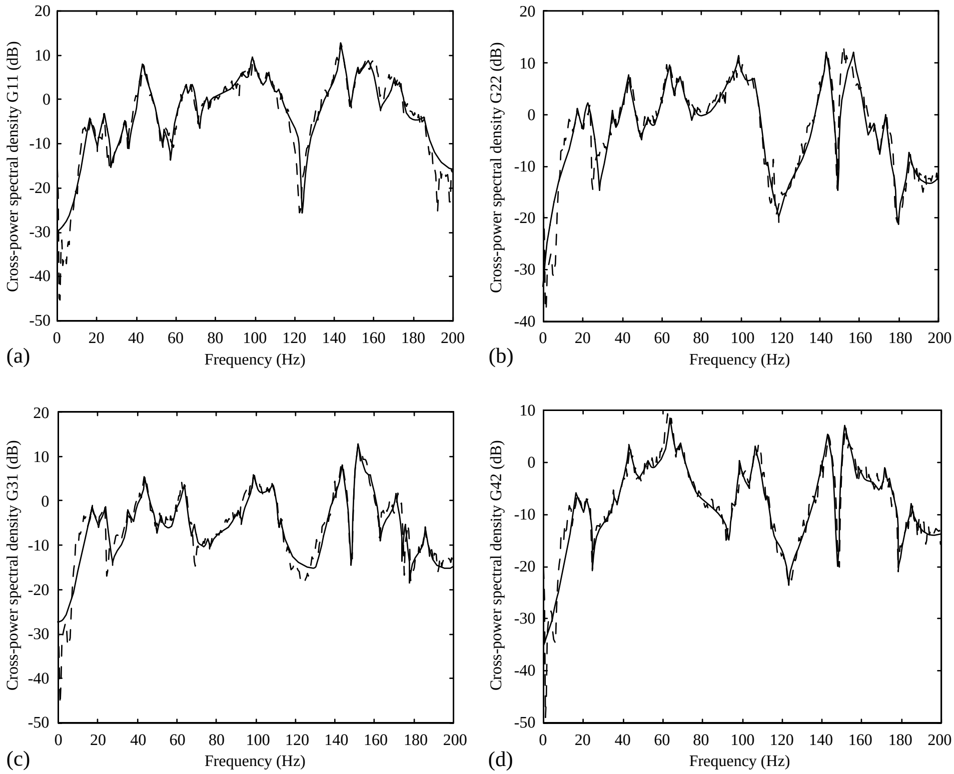

Figure 5. Comparison between measured (dashed line) and synthesized (solid line) power spectral densities. (a) Comparison between measured and synthesized auto-power spectral densities of point 1; (b) comparison between measured and synthesized auto-power spectral densities of point 2; (c) comparison between measured and synthesized auto-power spectral densities between point 3 and point 1 and (d) comparison between measured and synthesized auto-power spectral densities between point 4 and point 2.

The main features of the outlined frequency-domain poly reference modal identification method from only multi-output data can be summarized as follows:

(a) This method can obtain the global modal parameters of the system using all the measured data simultaneously. The system resonances are determinated by matrix operation not engineering skills.

(b) It does not require the modes of the structure to be sufficiently far apart. Some closely spaced modes of the vibration system can be identified well.

(c) It is convenient to check the quality of the modal parameters derived from the proposed technique by overlaying the synthesized auto- and cross-powers with the measured data.

(d) This technique based on that cross-correlation functions can be expressed in the same form as impulse response functions under the assumption of white-noise input forces.

(e) It is difficult to obtain reasonably accurate estimates for modal damping ratios of practical structures from response-only using the presented technique.

(f) When the total number of measured responses is greater than the number of the modes in the frequency range of analysis, singular value truncation technique can be adopted to reduce the model order if a drop between singular values is apparent. But for some practical reasons, the drop may become not apparent, the selection of the model order will become more complex and other techniques such as stabilization diagrams are needed to find the correct model order.

(g) It does not meet the strongly non-linear problem during the whole computing.

The good performance of the proposed frequency-domain technique has been shown in an experiment using an airplane model in this paper. Further investigation can be made of modal identification for practical large structures such as long-span bridges and tall buildings.

REFERENCES

1. L. Hermans, H. V. Auweraer, L. Mathieu and D. Coppens 1997 *Proceedings of the 15th IMAC*, 531–539. Modal parameter extraction from in-operation data.
2. E. Luz 1987 *Proceedings of the International Conference on Mechanical Dynamics*, 257–262. Experimental modal analysis of large-scale structures.
3. Z. W. Bao and J. M. Ko 1991 *The International Journal of Analytical and Experimental Modal Analysis* **6**, 57–68. Determination of modal parameters of tall buildings with ambient vibration measurements.
4. E. Luz and J. Wallaschek 1992 *The International Journal of Analytical and Experimental Modal Analysis* **7**, 29–39. Experimental modal analysis using ambient vibration.
5. T. J. Chalko and N. Haritos 1997 *Proceedings of the 15th IMAC*, 13–19. Scaling eigenvectors obtained from ambient excitation modal testing.
6. M. J. Desforges, J. E. Cooper and J. R. Wright 1995 *Mechanical Systems and Signal Processing* **9**, 169–186. Spectral and modal parameter estimation from output-only measurements.
7. N. Larbi and J. Lardies 2000 *Mechanical Systems and Signal Processing* **14**, 181–192. Experimental modal analysis of a structure excited by a random force.
8. D. Bonnecase, M. Prevosto and A. Benveniste 1990 *Proceedings of the 8th IMAC*, 382–388. Application of a multidimensional ARMA model to modal analysis under natural excitation.
9. D. Shi and W. Stuhler 1987 *Proceedings of the 5th IMAC*, 1171–1176. Modal analysis with AR (ARMA) model and unknown excitation.
10. P. Q. Zhang, Q. J. Yang, C. Q. Li and T. C. Huang 1990 *Proceedings of the 8th IMAC*, 819–826. An efficient identification method of modal parameters ARMAV model method.
11. L. Hermans and H. V. Auweraer 1999 *Mechanical Systems and Signal Processing* **13**, 193–216. Modal testing and analysis of structures under operational conditions: industrial application.
12. J. Lardies 1998 *Mechanical Systems and Signal Processing* **12**, 543–558. State-space identification of vibrating systems from multi-output measurements.
13. B. Peeters and G. De Roeck 1999 *Mechanical Systems and Signal Processing* **13**, 855–878. Reference-based stochastic subspace identification for output-only modal analysis.
14. L. Mevel, L. Hermans and H. Van Der Auweraer 1999 *Mechanical Systems and Signal Processing* **13**, 823–838. Application of a subspace-based fault detection method to industrial structures.
15. J. Lardies 2001 *Mechanical Systems and Signal Processing* **15**, 275–285. A stochastic realisation algorithm with application to modal parameter estimation.
16. G. H. James iii, T. G. Carne and J. P. Lauffer 1995 *Modal Analysis* **10**, 260–277. The natural excitation technique (NExT) for modal parameter extraction from operating structures.
17. G. H. James iii, T. G. Carne and R. L. Mayes 1996 *Proceedings of the 14th IMAC*, 77–83. Modal parameter extraction from large operating structures using ambient excitation.
18. D. Y. Chiang and M. S. Cheng 1999 *American Institute of Aeronautics and Astronautics Journal* **37**, 513–515. Modal parameter identification from ambient response.
19. L. M. Zhang, H. Kanda and F. Lembregts 1986 *Proceedings of the 4th IMAC*, 1237–1245. Some applications of frequency domain polyreference modal parameter identification method.
20. C. R. Zhou and C. S. Zhao 1989 *Parameter Identification for Mechanical Vibration and its Application*, 265–267. Peking: Science Books.

APPENDIX A: NOMENCLATURE

$[C]$	damping matrix
E	expectation operator
$\{f(t)\}$	vector of random forcing function
$f_l(t)$	white-noise input at the lth d.o.f.
$[G(j\omega)]$	auto- and cross-power spectral density function matrix between N and P responses which serve as references
$G_{np}(j\omega)$	cross-power spectral density function between the output n and the output p
$[G(j\omega)]_{redu}$	order-reduced cross-power spectral density matrix with dimension $N_e \times P$
$[h(t)]$	impulse response function matrix
$h_{nl}(t)$	impulse response function at the nth d.o.f. due to the input at the lth d.o.f.
$[\,]^H$	transpose and complex conjugate of matrix
$[H(j\omega)]$	frequency response function matrix
$H_{nl}(j\omega)$	frequency response function at the nth d.o.f. due to the input at the lth d.o.f.
$[I]$	unit matrix
$Im(\lambda_r)$	imaginary part of the rth eigenvalue λ_r
$[K]$	stiffness matrix
l	excitation point index
L	number of inputs
$[M]$	mass matrix
n	output point index
N	number of outputs
N_e	number of system modes in the frequency range of interest
N_m	number of system d.o.f.s
$\{0\}$, $[0]$	null vector, null matrix
p	response point index served as reference
P	number of references
$\{q(t)\}$	vector of modal co-ordinates
$q_r(t)$	rth component of modal co-ordinates vector $\{q(t)\}$
$[Q]$	constant matrix filled up with the term Q_{pr}
$[R(T)]$	auto- and cross-correlation function matrix
$R_{np}(T)$	cross-correlation function between the output n and the output p
$R_{npl}(T)$	cross-correlation function between two response signals $y_{nl}(t)$ and $y_{pl}(t)$
$Re(\lambda_r)$	real part of the rth eigenvalue λ_r
T	time separation
$[U]$	matrix composed of singular vectors of matrix $[Z]$
$[U_1]$	matrix containing the singular vectors corresponding to non-zero singular values of matrix $[Z]$
$[U_2]$	matrix containing the singular vectors corresponding to zero singular values of matrix $[Z]$
ω_k	kth discrete frequency in the measurement range
ω_{nr}	rth damped natural frequency
$[W]$	modal participation factor matrix
W_{lr}	modal participation factor
$[X]$	system matrix
$[X]_{redu}$	order-reduced system matrix with dimension $N_e \times N_e$
$\{y(t)\}$	vector of random displacements
$y_{nl}(t)$	response at the nth d.o.f. due to the input at the lth d.o.f.
$y_{pl}(t)$	response at the pth d.o.f. due to the input at the lth d.o.f.
$[Z]$	co-ordinate square difference matrix related to $[G(j\omega)]$
$\delta(t)$	Dirac delta function
$[\Lambda]$	complex eigenvalue matrix
λ_r	rth eigenvalue of the system
$[\phi]$	complex modal matrix
$[\psi]$	mode shape matrix of the system
$\{\psi_r\}$	rth mode shape vector of the system
ψ_{nr}	nth component of the rth eigenvector $\{\psi_r\}$
$[\psi]_{redu}$	order-reduced eigenvector matrix

ξ_r	damping ratio of the *r*th mode
$[\,]^{\mathrm{T}}$, $\{\,\}^{\mathrm{T}}$	transpose of matrix, vector
$[\,]^{+}$	generalized inverse of matrix
$[\Sigma]$	diagonal matrix containing the singular values of matrix $[Z]$ in descending order
$[\Sigma_1]$	matrix containing N_e non-zero singular values of matrix $[Z]$ in descending order
ε_1	the first non-zero singular value of matrix $[Z]$
ε_2	the second non-zero singular value of matrix $[Z]$
ε_{Ne}	the last non-zero singular value of matrix $[Z]$